Description of heavy ion collisions including the cascading of secondaries

Petr Závada
Department of High-Energy Physics, Institute of Physics, Czechoslovak Academy of Science, Na Slovance 2, CS-180 40 Prague 8, Czechoslovakia
(Received 25 September 1989; revised manuscript received 13 April 1990)

A simple Monte Carlo cascade model giving the exclusive description of the heavy ion collisions is described. Comparison with the data on O+Au collisions at 60 and 200 GeV suggests that in this energy region all secondary particles are produced basically by the multiple cascade collisions of the projectile and target nucleons, while the cascading of the produced particles is rather negligible.

I. INTRODUCTION

In the last few years considerable attention has been paid to the study of heavy ion collisions at high energies, see, e.g., Refs. 1 and 2 and references therein. The main aim of this effort is to find a signal of quark-gluon plasma, a new state of matter. Until now, the answer resulting from thorough analysis of the experimental data seems be rather negative, or at least it is getting obvious that the eventual signal, if any, is strongly mixed with the background resulting from processes of conventional hadron physics. For further analyses it is important to have a faithful description of the nucleus-nucleus collision without production of quark-gluon plasma, but properly accounting for all other peculiarities of hadron-nucleus and nucleus-nucleus collisions. In fact such a task represents an independent physical problem. The present paper concerns just this point.

The described approach is based exclusively on the classical notions of nuclear and high-energy hadron-nucleon phenomenology and consistent cascading procedure in three space dimensions. Actually, our Monte Carlo algorithm is a more general version of the cascade model of hadron-nucleus interactions proposed earlier.[3,4] The difference between our model and known string models, e.g., FRITIOF (Ref. 5) is first of all on the level of description of single hadron-nucleon interaction. While in string models secondary particles resulting from individual collisions are created by the fragmentation of the color strings; our single collision generator does not contain any refined physics on the level of quarks, but is rather a simple parametrization of basic features of hadron-nucleon interactions. In our approach the secondary particles resulting from the hadron-nucleon collision are assumed to have a common pointlike origin. The probability of their next interaction is controlled by the formation time, which is the only free parameter of our approach. Due to very simplified dynamics of hadron-nucleon interactions, our approach enables relatively easily to take into account consistently the cascading of the secondaries. In the FRITIOF model and in some other models[6,7] in which more fundamental hadron-nucleon generators are used, the incorporation of cascading initiated by the secondary particles is less consistent or absent entirely. Moreover, our resulting Monte Carlo algorithm is sufficiently simple and transparent but simultaneously general enough to enable easily to check the sensitivity of various generated spectra with respect to the assumptions relevant for the description of nucleus-nucleus collisions.

The outline of the paper follows. The generator of hadron-nucleon interaction is described in Sec. II. The simulation of nucleus-nucleus collision including the cascading of the secondaries is described in Sec. III. In Sec. IV the calculated distributions are compared with the data of the NA35 experiment, and the last section is devoted to the discussion and summary of the results.

II. GENERATOR OF HADRON-NUCLEON COLLISION

For simplicity our generator of hadron-nucleon interactions[8] used in the Monte Carlo for nucleus-nucleus collisions gives only two kinds of secondaries: the leading particles having the same masses and charges as the initial ones (projectile+nucleon) and produced particles treated as pions and considered with equal probability as π^-, π^+, and π^0. The simulated events are unweighted, having the distributions obeying the following phenomenological relations.

(1) Differential cross sections are as follows.

Inelastic:

$$\frac{d\sigma_{\text{in}}}{dp_T^2} \sim \exp(-\beta p_T^2) , \tag{1}$$

$$\frac{d\sigma_{\text{in}}}{dx_F} \sim (1-|x_F|)^{\alpha}, \quad \text{for produced particles}$$

$$\frac{d\sigma_{\text{in}}}{dx_F} \sim \text{const}, \quad \begin{array}{l} \text{projectile: } 0<x_F<1 \\ \text{recoiled nucleon: } -1<x_F<0 \end{array} \tag{2}$$

where $x_F = p_L / p_{\max}$ in c.m.s.

Elastic:

$$\frac{d\sigma_{\text{el}}}{dt} \sim \exp(\gamma t) . \tag{3}$$

Integral cross sections depend on the energy:[9]

$$\sigma(s) = a_1 + a_2 s^{-b} + a_3 \ln^2(s), \quad \sqrt{s} > 3 \text{ GeV} . \tag{4}$$

TABLE I. The parameters used in the hadron-nucleon generator. The values relevant for the "average" nucleon (N) are obtained as an average of those corresponding to proton and neutron.

Collision	Mean charged multiplicity A_1	A_2	A_3
πN	0.865	0.777	0.069
NN	0.830	0.467	0.115

Collision	Integral cross section a_1	a_2	a_3	b
Total πN	17.7	29.6	0.136	0.502
Total NN	30.8	26.1	0.170	0.418
Elastic πN	1.38	14.4	0.034	0.520
Elastic NN	4.50	42.0	0.045	0.682

α	Differential cross sections β (c^2/GeV^2)	γ (c^2/GeV^2)
1.5–13.0	7.0	1.0–11.0

A modification of the cross sections in the low energy region is made in accordance with Ref. 10.

(2) Charged multiplicity distribution is as follows:[11]

$$P(z)=(3.79z+33.7z^3-6.64z^5+0.332z^7)\times\exp(-3.04z),\quad z=n/\langle n\rangle\ . \tag{5}$$

Mean charged multiplicity depends on the energy:[9]

$$\langle n\rangle=A_1+A_2\ln(s)+A_3\ln^2(s)\ . \tag{6}$$

Numerical values of the relevant constants are listed in Table I. The value α depends on the multiplicity and also, due to the used procedure of generation, slightly on $|x_F|$. The approximation of energy-dependent γ is based on the tables in Ref. 10.

The generator of this kind gives a simplified description of hadron-nucleon collisions, which, however, is for our purpose fully sufficient since the generated spectra agree well with the experimental data.[4]

III. SIMULATION OF NUCLEUS-NUCLEUS COLLISIONS

Similarly as in other models, the collision of the two nuclei is in our approach postulated as a noncoherent superposition of the hadron-nucleus collisions. The hadrons are either nucleons forming initial nuclei or eventually secondaries developing intranuclear cascades. The Monte Carlo procedure can be formulated as follows.

(1) First of all, impact parameter of the whole projectile and the positions of single nucleons in the region intersecting the target nucleus are generated according to a standard nuclear density distribution:

$$\rho(r)=\frac{\rho_0}{1+\exp[(r-r_A)/c]},\quad c=0.54$$
$$r_A=1.19A^{1/3}-1.61A^{-1/3}\ , \tag{7}$$
$$\rho_0=A\left[\frac{3}{4\pi}r_A^{-3}\right]/(1+c^2\pi^2/r_A^2)\ .$$

At this stage the corresponding Fermi momenta are generated as well. The positions of target nucleons are generated analogously.

(2) Making projections of the projectile onto the target in the beam direction, the ordered sequences of target nucleons with which each of the projectile nucleons is expected to interact is obtained. The order is apparent from Fig. 1(a): first of all the most forward nucleon X of the projectile is traced through the target, afterwards the next most forward one Y follows, etc. Interactions are assumed to take place for the pairs of nucleons separated by less than $d=\sqrt{\sigma_{PP}/\pi}$ in the transversal plane, where σ_{PP} is the total cross section for nucleon-nucleon interaction. At this stage σ_{PP} is assumed to be constant having the value corresponding to the initial nucleon energy, ignoring the fact that the energy of the projectile nucleon and the cross section correspondingly can vary during the passage through the target.

(3) The collisions of the projectile nucleons with the target ones are simulated by the generator described in the preceding section. Although in general both projectile and target nucleons interact several times, changing their momenta at each collision, their positions in respective nuclei rest frames are for the sake of simplicity kept frozen. Resulting momenta and the starting positions of created pions and recoiled nucleons are kept in the memory until the collisions of the last projectile nucleon are generated.

(4) After the whole projectile nucleus passed through the target, the secondary particles resulting from individual collisions generated according to rule (3) are traced through it too. The development of cascades is apparent from Fig. 1(b), where the following rule holds: first of all the particles coming from first interaction point are in decreasing order of their $p_{\rm lab}$ traced in the target until the next collision or until reaching the nuclear boundary. The new interaction points are numbered consecutively. Then the particles coming from the second, third, etc., interaction points are processed in the same way until exhausting all the interaction points.

The tracing consists of sufficiently small steps Δl in the direction of the momentum and the probability p of interaction at each step depends on corresponding cross section σ and local nuclear density ρ:

$$p=\sigma\rho\Delta l\ . \tag{8}$$

Values of σ [see relation (4)] are assumed to be the same as for hadron-nucleon interaction outside the nuclear environment. The formation length plays the same role as in the hadron-nucleus case,[4] i.e., the secondary hadron is allowed to interact only after passing the distance l generated according to the formula:

$$P(l)dl \sim \exp(-l/l_f)dl, \quad l_f = \tau \frac{p_{\text{lab}}}{m} , \tag{9}$$

where τ is proper formation time, p_{lab} and m are the momentum and mass of the created particle. It is obvious that cascading in the region of intersection of the target with the projectile requires a special treatment. In the present approach it is assumed that recoiled nucleons and created pions can interact only with those target nucleons which have not been touched by the projectile, and any mutual interaction of the secondaries is excluded. For this reason the nuclear density entering the probability (8) of cascade collision is reduced inside the intersection by the factor

$$c_{\text{red}} = (1 - n_{\text{act}}/n_{\text{in}}) , \tag{10}$$

where n_{act} is the number of active target nucleons and n_{in} is the total number of target nucleons in the region of intersection, see Figs. 1(a) and (b). This approach to trailing effect is very approximate, but more generally, the factor c_{red} could be within certain limits considered as a

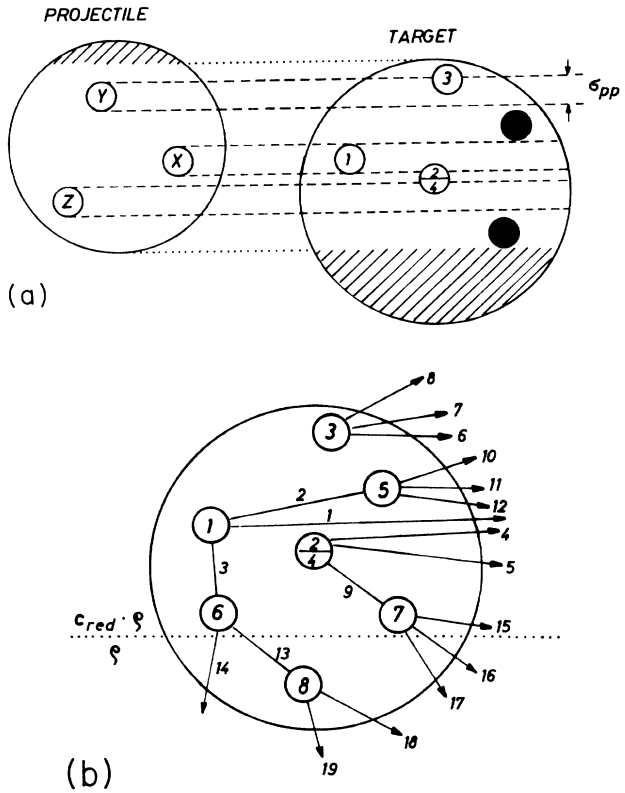

FIG. 1. (a) Schematic display of the two nuclei interaction as the multiple collision of projectile and target nucleons. The open circles represent the active projectile and target nucleons. The numbers inside the target nucleons define the order for the generation of single collisions. The circle with the two numbers corresponds to the nucleon that is struck twice. The full circles represent passive target nucleons in the region of intersection. (b) Schematic display of the intranuclear cascades starting at the primary interaction vertexes. For the numbering of single links see text. The dotted line represents a boundary of the intersection.

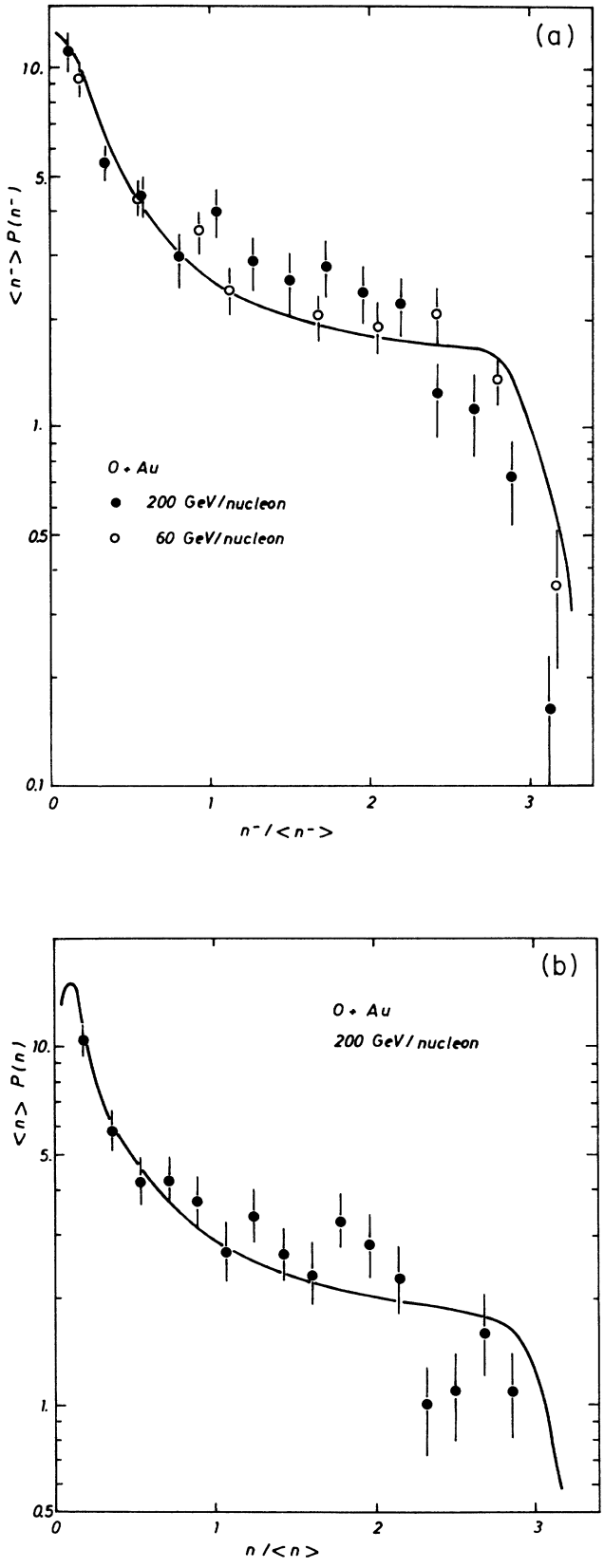

FIG. 2. The multiplicity distribution of negative (a) and charged (b) particles produced in the region $\vartheta < 60°$ for minimum bias trigger. The circles correspond to the experimental data, the solid line is the result of simulation.

free parameter. Inside the nucleus no distinction between the protons and neutrons is made, but when leaving the target nucleus the outgoing nucleons are randomly defined as protons or neutrons, taking into account only the mass and atomic numbers of the target nucleus. The analogous rule is applied for the active projectile nucleons as well.

(5) In the present approach the cascading is simulated in target nucleus only, i.e., the projectile is assumed to be a rather lighter nucleus and the target a rather heavier one.

Remaining details relevant for consistent accounting of nuclear environment as Fermi motion and Pauli blocking are included into the procedure exactly in the same way as in Refs. 3 and 4.

IV. RESULTS

The results of the calculation are compared with the data of the experiment NA35 on O+Au collisions at 60 and 200 GeV/nucleon,[12,13] trying different assumptions concerning the cascading and the formation length of produced particles.

First of all, the cascading approach,[4] fitting well the hadron-nucleus collisions, is checked for nucleus-nucleus interaction as well. In the latter case it can be formulated as follows.

(a) Only nucleons forming projectile and target are allowed to develop cascades inside the target, while pions resulting from the cascades are prevented to interact within the nucleus. The formation length of leading nucleons is supposed to be $l_f = 0$. The following results are obtained using consistently the same kinematical cuts in the Monte Carlo as in the experiment.

In Fig. 2(a) the comparison of negative particle multiplicity distributions in terms of the scaling variable $n^-/\langle n^- \rangle$ is shown. The experimental values are slightly different for both data sets, while calculated curves for both energies coincide within the statistical errors ($\sim$20 000 generated events for each energy), therefore their average is shown in the figure. It is seen that the calculated shape of the distribution fits the data very well at 60 GeV, while for 200 GeV the agreement is slightly worse. For mean multiplicities the agreement is very good for both energies, see Table II.

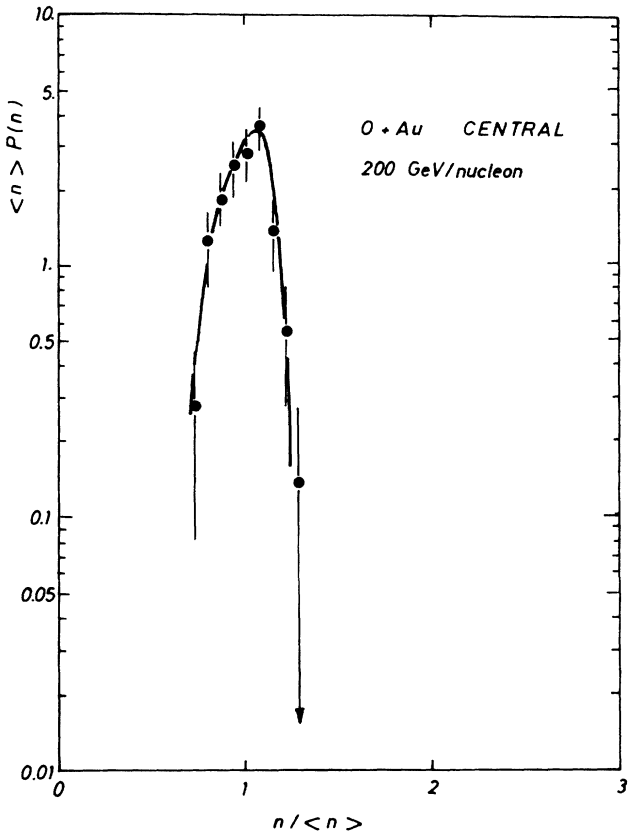

FIG. 3. The multiplicity distribution of charged particles produced in the region $\vartheta < 60°$ for forward energy veto trigger.

Figure 2(b) shows the comparison of the multiplicity distribution of the all charged particles at 200 GeV/nucleon. The shape of the calculated curve agrees with the data qualitatively well, but some quantitative disagreement is apparent especially for high multiplicity tail. However, the average values agree very well again (Table II).

Figures 3 and 4 concern central collisions O+Au at 200 GeV. The term "central" here means the application of "forward energy veto trigger".[13,14] Multiplicity distribution of charged particles is shown in Fig. 3. The shape

TABLE II. The comparison of experimental and calculated mean values of the multiplicity and rapidity distributions in Figs. 2–4.

		Minimum bias data		Central collision data
		60 GeV	200 GeV	200 GeV
$\langle n^- \rangle$	Expt.	27.0±1.2	45.6±1.6	124±2
	Calc.	27.07	46.46	132.3
$\langle n \rangle$	Expt.	69.9±2.8	111±4	286±4
	Calc.	69.54	109.7	311.5
$\langle y \rangle$	Expt.			2.43±0.01
	Calc.			2.46

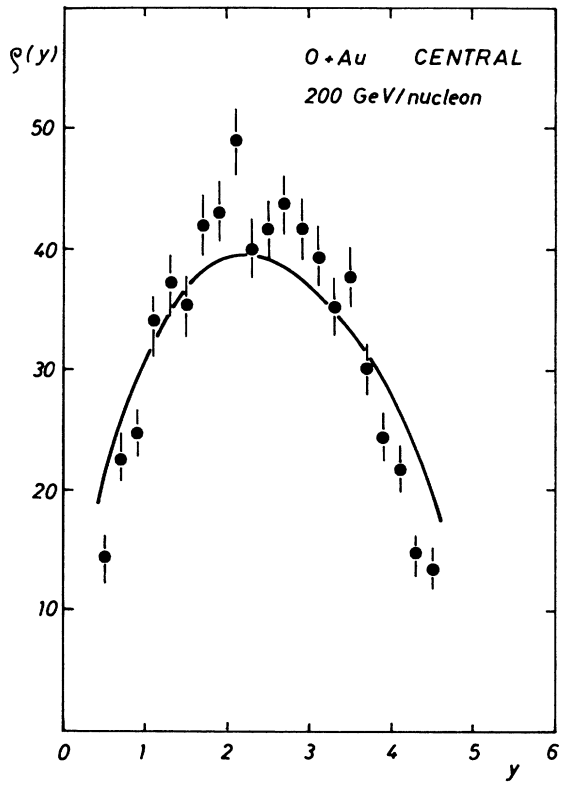

FIG. 4. The rapidity distribution of negative particles with the momenta $p_{\text{lab}} > 0.1$ GeV/c and $p_T < 2$. GeV/c is for forward energy veto trigger.

of calculated curve fits the data fairly well, but the corresponding mean value is slightly higher (by 9%) than the experimental one (Table II).

Figure 4 shows the comparison of rapidity distribution

$$\rho(y)=\frac{1}{N_{\text{ev}}}\frac{dN}{dy} \tag{11}$$

of negative particles resulting from central O+Au collisions. The calculated curve is normalized to the experimental data. The calculation gives apparently a broader distribution (dispersion $D=(\langle y^2\rangle-\langle y\rangle^2)^{1/2}$ is by 8% greater). However the average rapidity is reproduced very well (Table II).

To check how the calculated distributions are sensitive with respect to the input values of l_f, the following two versions of the calculation have been performed.

(b) In distinction to the version (a), it was assumed that created pions can develop intranuclear cascades inside the target. For this calculation the mean value of pion proper formation time was taken to be $\tau=1$ fermi. Formation length of the nucleons (or leading pions from interactions initiated by produced pions) remains the same as in the version (a), $l_f=0$. In this point the considered version differs from the version (b) in Ref. 4 for the hadron-nucleus case, where the distribution (9) has been applied for all secondary particles, including the leading nucleons.

(c) The cascading of recoiled nucleons and created pions is suppressed completely, all secondary particles being produced only by rescattering of projectile nucleons inside the target.

The average multiplicities corresponding to all three versions (a), (b), and (c) are listed in Table III. First of all, comparison with the experimental data on $\langle n^-\rangle$, $\langle n\rangle$ summarized in Table II, proves that version (a) (in which only nucleons are allowed to develop the cascading) gives best agreement with the experimental data. This conclusion is fully consistent with the results of the previous study of proton-nucleus interactions.[4] On the other hand the version (b) gives slightly higher average multiplicities in the region of the acceptance. It is however apparent that, in particular, negative multiplicities are, in this region ($\vartheta < 60°$), not very sensitive to the pion cascading. This is due to the fact that the cascading is controlled by the relation (9) according to which the secondary interactions of particles with higher momenta being produced predominantly in a narrow forward cone are suppressed. The influence of pion cascading is more pronounced, if also fragmentation region of the target is taken into account, see lower part of Table III. Finally, results of calculation (c) compared with (a) show that the cascading of recoiled nucleons contributes $\sim 20-30\%$, depending on the angular acceptance, of resulting charged multiplicity. This contribution is important and obviously the agreement of version (c) with the experimental data is the least satisfactory.

V. DISCUSSION AND SUMMARY

In this paper we presented simple Monte Carlo cascade model and the comparison of its predictions with the experimental data on O+Au collisions at 60 and 200 GeV/nucleon.

We studied three distinct approaches accounting for secondary particle cascading and came to the conclusion that cascading of recoiled nucleons, ignored in some

TABLE III. The mean values of the multiplicity distributions calculated with various assumptions [(a)–(c), see text] concerning the cascading of secondaries for minimum bias trigger. Values $\langle n^-\rangle$, $\langle n\rangle$ correspond to the region $\vartheta < 60°$; $\langle n_{\text{all}}^-\rangle$, $\langle n_{\text{all}}\rangle$ are evaluated without angular cuts.

	60 GeV			200 GeV		
	(a)	(b)	(c)	(a)	(b)	(c)
$\langle n^-\rangle$	27.07	27.60	22.98	46.46	49.22	38.16
$\langle n\rangle$	69.54	77.23	55.34	109.7	123.8	85.84
$\langle n_{\text{all}}^-\rangle$	30.77	34.36	25.29	50.39	57.24	40.16
$\langle n_{\text{all}}\rangle$	85.01	106.2	60.98	126.1	156.9	90.88

models, e.g., the FRITIOF, can give a significant contribution to the resulting multiplicities. Concerning the approach with cascading of the produced pions, our computation with input value $\tau = 1$ fermi has shown that in the considered region of primary energy and geometrical acceptance ($\vartheta < 60°$) its contribution to the resulting charged multiplicity is rather small. A more sensitive test of effect of produced particle cascading should be done with the data covering a significant part of the target fragmentation region.

In accordance with our previous study on proton-nucleus collisions, the best agreement with the experimental data has been achieved in the approach (a) in which only nucleons forming the initial nuclei develop intranuclear cascades, while the formation length of the produced pions exceeds the nuclear dimension. For the minimum bias event sample we obtained in this approach a good agreement for multiplicity distributions of negative and charged particles at 60 and 200 GeV/nucleon. As far as the corresponding average values are concerned, the agreement is excellent. In the case of central collisions the calculated mean value of the charged multiplicity distribution is by 9% higher than the experimental one. The average rapidity of negative particles in this event sample is reproduced very well, but the calculated distribution is slightly broader.

Our statement concerning the absence of pion cascading in both hadron-nucleus and nucleus-nucleus interactions is not in accordance with the claim of some authors, e.g., Refs. 6 and 15, that pion cascading plays an important role. On the other hand, there are other models (FRITIOF) that also assume produced particles to be formed behind the nucleus. The authors of the recent paper,[16] analyzing the data on multiparticle production by π^+, K^+ on gold, silver and magnesium targets at 200 GeV, come to the same conclusion.

It is obvious that the effect of the produced particle cascading and correspondingly the formation length is still not well understood. Consequently, the predictions of various models aspiring to unique description of hadron-nucleus and nucleus-nucleus interactions should be consistently confronted with existing experimental data. The question of space-time scale for hadron creation is interesting by itself, but in addition it is obvious, that the correct estimation of background spectra resulting from high energy hadron physics is essential for correct evaluation of the new interesting effects in relativistic nuclear physics like the production of quark-gluon plasma.

ACKNOWLEDGMENTS

I would like to express my gratitude to Professor Ivo Derado for stimulating discussions and warm hospitality during my stay at NA35 group of MPI-Munich, where the basic part of this paper has been done.

[1]Proceedings of the Sixth International Conference on Ultra-Relativistic Nucleus-Nucleus Collisions-Quark Matter 1987, Nordkirchen, 1987 [Z. Phys. C **38**, 1 (1988)].

[2]*Proceedings of the International Conference on Physics and Astrophysics of Quark-Gluon Plasma,* Tata Institute of Fundamental Research, Bombay, India, 1988, edited by Bikash Sinha and Sibaji Raha (World Scientific, Singapore, 1989).

[3]P. Závada, Z. Phys. C **32**, 135 (1986).

[4]P. Závada, Phys. Rev. C **40**, 285 (1989).

[5]B. Nilsson-Almqist and E. Stenlund, Comput. Phys. Commun. **43**, 387 (1987); B. Andersson, G. Gustafson, G. Ingelman, and T. Sjöstrand, Phys. Rep. **97**, 31 (1983); B. Andersson, S. Garpman, G. Gustafson, H.-A. Gustafsson, B. Nilsson-Almqvist, I. Otterlund, and E. Stenlund, Phys. Scripta **34**, 451 (1986); B. Andersson, G. Gustafson, and B. Nilsson-Almquist, Lund University Report LU-TP 86-3, Lund, Sweden (1986).

[6]J. Ranft, Phys. Rev. D **37**, 1842 (1988).

[7]J. M. Shabelsky, Yad. Fiz. **50**, 239 (1989).

[8]P. Závada (unpublished).

[9]V. Šimák and J. Vávra, Z. Phys. C **35**, 517 (1987).

[10]J. Bystricky *et al.*, in *NN and KN Scattering,* Vol. I/9a of *Landolt-Börnstein, New Series,* edited by H. Schopper (Springer, Berlin, 1980); G. Höhler, in *πN Scattering,* Vol. I/9b of *Landolt-Börnstein, New Series,* edited by H. Schopper (Springer, Berlin, 1982).

[11]P. Slattery, Phys. Rev. Lett. **29**, 1624 (1972).

[12]A. Bamberger *et al.*, Phys. Lett. B **205**, (1988); **205**, 583 (1988).

[13]A. Bamberger *et al.*, Z. Phys. C **38**, 89 (1988).

[14]I. Derado, private communication.

[15]B. B. Levchenko and N. N. Nikolaev, Yad. Fiz. **37**, 1016 (1983); Yad. Fiz. **42**, 1255 (1984).

[16]D. H. Brick *et al.*, Phys. Rev. D **39**, 2484 (1989).